Journal of Advanced Ceramics
2012, 1(1): 72-78
DOI: 10.1007/s40145-012-0008-y ISSN 2226-4108
Research Article

Significant photocatalytic enhancement in methylene blue degradation of Bi_2WO_6 photocatalysts via graphene hybridization

Feng ZHOU [a,b,*], Yongfa ZHU [b]

[a] *Department of Materials Science and Engineering, Dalian Maritime University, Dalian 116026, China*
[b] *Department of Chemistry, Tsinghua University, Beijing 100084, China*

Received September 1, 2011; Accepted November 22, 2011

Abstract: The hybridization of graphene with Bi_2WO_6 photocatalysts was employed to enhance the photocatalytic activity. The photocatalytic activity enhancements were dependent on the amount of graphene and it was found that the optimal hybridized amount of graphene was about 1.5 wt%, which was close to the monolayer dispersing of graphene on Bi_2WO_6 surface. Up to four times of the photocatalytic activity was enhanced by the hybridization of graphene, compared with that of pristine Bi_2WO_6. The enhancement mechanism of the photocatalytic activity was attributed to the higher separation efficiency and the inhibition of recombination of photoinduced electron-hole pairs. The electronic interaction was verified by the photoelectrochemical measurements.

Key words: powders-chemical preparation; carbon; nanocomposites; photocatalyst

1 Introduction

In the past few decades, semiconductor-based photocatalysis has attracted extensive interest, and TiO_2 is considered as one of the best photocatalysts for environmental remediation due to its higher photocatalytic activity, good chemical stability, non-toxicity and low cost [1-6]. However, due to its large bandgap (3.2 eV), TiO_2 can only absorb UV light, which occupies only about 4% of the solar energy [7]. Therefore, it is important to develop visible-light responsive photocatalysts, which is drawing more and more attention recently. Bi_2WO_6 is found to be a potential excellent photocatalyst because of its unique molecular and electronic versatility, reactivity, stability, etc [8-10]. By a typical hydrothermal process, Bi_2WO_6 nanoplates were capable of fast separation and transfer of photo-generated electrons and holes [8]. How to design more efficient Bi_2WO_6-based photocatalysts remains a huge challenge.

Many works have been devoted to improve the separation of photogenerated electron-hole pairs by coupling the photocatalysts with carbon materials [11-12]. The authors have developed the carbon material hybridized semiconductor as efficient photocatalysts, such as C60 [13], graphite-like carbon [14,15], graphene-like carbon [16] and graphene [17,18]. Thus, a combination of Bi_2WO_6 and graphene is promising to simultaneously possess excellent transparency, conductivity, and controllability, which could facilitate effective photodegradation of pollutants under visible light.

* Corresponding author.
E-mail: zhoufeng99@mails.tsinghua.edu.cn

To the authors' best knowledge, there are only few reports focused on this topic [19-20]. However, the mechanism of the electronic interaction between graphene and semiconductor is still unclear and need further studies. Herein, the authors demonstrated a facile route to obtain an efficient graphene-hybridized Bi_2WO_6 photocatalyst. It is found that the hybridization with an appropriate amount of graphene could significantly improve the photodegradation property of Bi_2WO_6 under visible light irradiation. It is postulated that the enhanced photoactivity of Bi_2WO_6 by graphene hybridization results from high migration efficiency of photoinduced electron-hole pairs. The structure and interfacial electronic interaction between Bi_2WO_6 and graphene, as well as its effect on the photocatalytic activity were systematically investigated.

2 Experiments

2.1 Materials preparation

Bi_2WO_6 was synthesized by the hydrothermal method. In a typical procedure, 10 mmol of $Na_2WO_4 \cdot 2H_2O$ and 20 mmol of $Bi(NO_3)_3 \cdot 5H_2O$ were respectively dissolved in 150 mL of distilled water, and then transferred into a 160 mL Teflon-lined stainless steel autoclave. The autoclave was sealed and maintained at 180℃ for 24 h, then cooled to room temperature naturally. Graphene oxide (GO) was produced from nature graphite by the Hummers method [21]. All the chemicals used were reagent grade without further purification. Preparation of graphene-hybridized Bi_2WO_6 was prepared in two steps. Firstly, appropriate as-prepared graphite oxide was dispersed in water to achieve a 0.05 wt% dispersion. Exfoliation of graphite oxide to GO was obtained by ultrasonication of the dispersion for 30 min and 1 g Bi_2WO_6 was added into the GO dispersion. Then Bi_2WO_6 and GO mixture was dispersed by ultrasonication for 30 min and stirred for 24 h. The suspension was filtrated and the precipitate was washed with deionized water three times, and then transferred to an oven to dry at 60℃ for 24 h; according to this method, different mass ratios of GO-Bi_2WO_6 powders from 0.5 to 4.0 wt% were synthesized. The second step was the reduction of GO to graphene which was performed according to the literature [22,23]. Appropriate GO-Bi_2WO_6 powder was dispersed in water and ultrasonicated for 30 min. In a typical procedure, appropriate amount of hydrazine solution (35 wt% in water) and ammonia solution (28 wt% in water) were added to the above dispersion. The weight ratio of hydrazine to GO was about 7:10. After being shaken or stirred for a few minutes, the dispersion was put in a water bath (95℃) for 1 h. Finally, graphene-hybridized Bi_2WO_6 was obtained after evaporated at 60℃ for 24 h.

2.2 Characterization

The diffusion reflection spectra (DRS) measurements of the samples were recorded on a Hitachi U-3010 instrument with $BaSO_4$ as the reference sample. High resolution transmission electron microscopy (HRTEM) images were obtained by JEM 2010F field emission transmission electron microscope with an accelerating voltage of 200 kV.

2.3 Photocatalytic experiments

The photocatalytic activities of the as-prepared samples were evaluated by the degradation of Methylene Blue (MB) under visible light irradiation ($\lambda > 420$ nm). The visible light was obtained by a 500 W xenon lamp (Institute of Electric Light Source, Beijing) with a 420 nm cutoff filter to ensure that the desired irradiation light was obtained. The average light intensity was 30.8 $mW \cdot cm^{-2}$ measured by a power meter from the Institute of Electric Light Source, Beijing. 50 mg of graphene-hybridized Bi_2WO_6 samples were dispersed in a 100 mL MB suspension (1×10^{-5} M). The suspensions were magnetically stirred in the dark for 30 min to reach the absorption-desorption equilibrium before the irradiation. At certain time intervals, 3 mL aliquots were sampled and centrifuged to remove the particles. The filtrates were analyzed by recording variations in the absorption band (664 nm) in the UV-visible spectra of MB using a Hitachi U-3010 UV-Vis spectrophotometer. The active species generated in the photocatalytic system could be detected through trapping by ethylenediamine tetraacetic acid disodium salt (EDTA-Na) and *tert*-butyl alcohol (*t*-BuOH).

2.4 Photoelectrochemical measurements

Photoelectrochemical performances were measured on an electrochemical system (CHI-660B, China). The ITO/Bi_2WO_6 or ITO/Graphene-Bi_2WO_6 electrodes served as the working electrode. The counter and the reference electrodes were platinum gauze and saturated calomel electrode (SCE), respectively. A 500 W xenon lamp with a 420 nm cutoff filter was used as the source of visible light irradiation. The photoresponses of the photocatalysts as visible light on and off were measured at 0.0 V.

3 Results and Discussion

3.1 Enhancement of photocatalytic activity and photocurrents

The photocatalytic activities of Graphene-Bi_2WO_6 (G-BWO) photocatalysts were measured by the photodegradation of MB as model reaction under visible light ($\lambda > 420$ nm), and the results were shown in Fig. 1. It can be seen in Fig. 1a that visible light activity has been enhanced for all the Graphene-Bi_2WO_6 samples, compared to the reference photocatalyst. The reference photocatalyst had poor photocatalytic activity and it could degrade only about 43.4% MB within 2 h. By contrast, the Graphene-Bi_2WO_6 (1.5 wt%) photocatalyst exhibited the highest activity and it could degrade MB by 88.1% within 2 h. Figure 1a also showed that an increasing in the graphene content did not improve monotonously the photocatalytic performance of Graphene-Bi_2WO_6. When the graphene content was relatively low (< 1.5 wt%), the photocatalytic activity increased monotonously. However, when the graphene content was relatively high (> 1.5 wt%), the photocatalytic activity decreased with increasing graphene content. According to Fig. 1a, the optimal loading amount of graphene on the surface of BWO was approximately 1.5 wt%. The decrease in photocatalytic activity at higher graphene loading amount was attributed to the increased absorbance and scattering of photons through excess graphene in the photosystem. It is well recognized that the photocatalytic degradation of organic pollutants follows pesudo-first-order kinetics [24]. In this system, it can be explained by a Langmuir-Hinshelwood model. The apparent reaction rate constants (k) for the degradation of MB can be derived from the linear slope of the relationship between $\ln(C/C_0)$ and t, where C_0 and C are the concentrations of initial solution and after t (min) of irradiation, respectively. Figure 1b presented the photodegradation rates of MB on graphene, Bi_2WO_6, Graphene-BWO composite (1.5 wt%), and mechanical blend of Bi_2WO_6 and graphene. Pure Bi_2WO_6 had an apparent reaction rate constant k of 0.0047 min^{-1}, while graphene showed negligible photodegradation of MB. Graphene-BWO composite sample showed the highest activity (k=0.0176 min^{-1}), the activity of MB degradation was enhanced by almost four times after 1.5 wt% of graphene loaded. Noticeably, the mechanical blend of Bi_2WO_6 and graphene (1.5 wt%) showed slightly higher photocatalytic activity than that of pure Bi_2WO_6. The four times enhancement in activity of Graphene-BWO composite compared with mechanical mixture of Bi_2WO_6 and graphene was attributed to the intimate contact between Bi_2WO_6 and graphene, which was crucial for the formation of electronic interaction and interelectron transfer at the interface.

Photoelectrochemical experiments were carried out

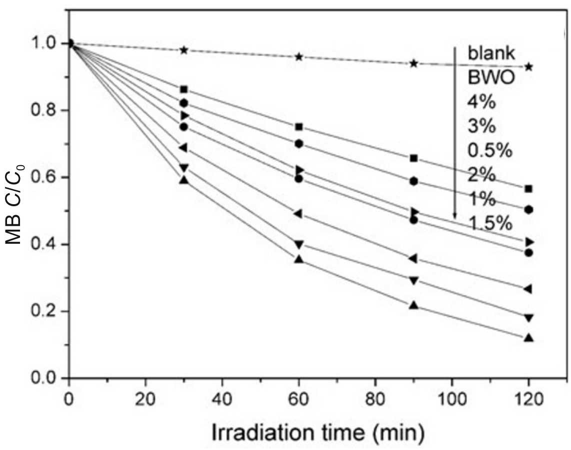

(a)

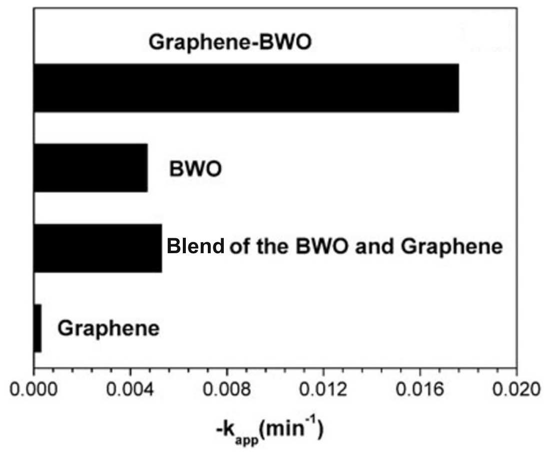

(b)

Fig. 1 Photocatalytic degradation of MB over the as-prepared samples under visible light irradiation ($\lambda > 420$ nm): (a) the photodegradation plots and rate constant k as a function of graphene content, (b) the apparent rate constant of MB photodegradation on graphene, BWO, mechanical mixture of BWO and graphene (1.0 wt%), and the Graphene-BWO (graphene 1.5 wt%) composite, catalyst loading, 0.5 $g \cdot L^{-1}$; MB, 1×10^{-5} M to investigate the electronic interaction between Bi_2WO_6 and graphene. Photoresponses were performed for Graphene-Bi_2WO_6 (1.5 wt%) and Bi_2WO_6 after deposition on ITO electrodes (Fig. 2). A fast and uniform photocurrent response was observed for each switch-on and -off event in both electrodes (Graphene-Bi_2WO_6 and Bi_2WO_6). The photocurrent transients had almost the same shape for each electrode. This photoresponsive phenomenon was entirely reversible. It was worthy to note that the photocurrent of the Graphene-Bi_2WO_6 electrode was about six times of that for the Bi_2WO_6 electrode. This was consistent with the degradation experiment, and clearly indicated that the hybridization can improve the separation efficiency of photoinduced electrons and holes. The electron transfer from photocatalysts to the graphene sheet had been detected by time-resolved fluorescence spectroscopy in the Graphene-CdS nanocomposite [25].

An attractive feature of the photocatalyst materials was that the photocatalytic activity of the photocatalyst was stable. To evaluate the stability of the photocatalyst, the recycled experiments for the photodegradation of MB were performed, and the results were shown in Fig. 3. Under visible light irradiation, 88.1% of MB could be degraded over Graphene-Bi_2WO_6 (1.5 wt%) within 2 h for the first irradiation, and the samples presented stable visible light photocatalytic activity in the recycled reaction. The stability of the photocatalyst was attributed to the chemical interaction between Bi_2WO_6 and graphene, which enable the graphene stable to the photocatalyst, and the graphene cannot be degraded during the photodegradation of MB.

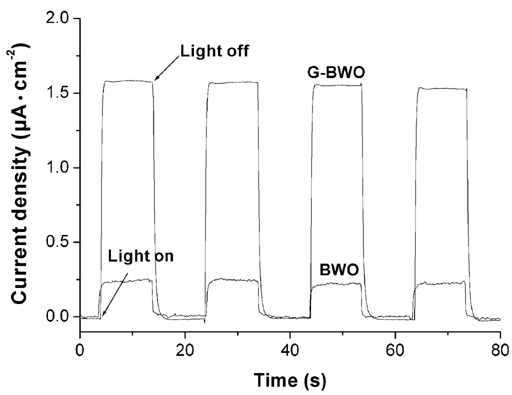

Fig. 2 Photocurrent transient responses of BWO and G-BWO electrodes. [Na_2SO_4]=0.1 M

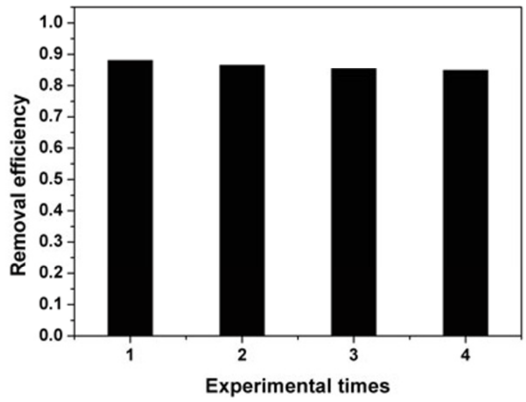

Fig. 3 Removal efficiency of MB with experimental times in the presence of graphene-BWO photocatalyst under visible light irradiation ($\lambda > 420$ nm)

3.2 Hybrid structures

DRS patterns of Graphene-Bi_2WO_6 photocatalysts were shown in Fig. 4. As expected, pure Bi_2WO_6 showed the characteristic spectrum with its fundamental absorption sharp edge rising at 470 nm, while the Graphene-Bi_2WO_6 samples absorbed in the whole visible region due to the presence of graphene on Bi_2WO_6. The absorption edge of Bi_2WO_6 can also be detected in Graphene-Bi_2WO_6 samples. With the loading of graphene, the Graphene-Bi_2WO_6 samples displayed the same absorption edge as that of Bi_2WO_6. The absorption intensity of the samples varied with the increased amount of the graphene. Furthermore, the absorbance of samples at the wavelength of 600 nm changed with mass ratio of graphene/BWO (the inset of Fig. 4). The absorption intensity increased rapidly with the ratio of graphene/Bi_2WO_6 from 0.5 to 1.5 wt%, but the increment was insignificant from 1.5 to 4 wt%.

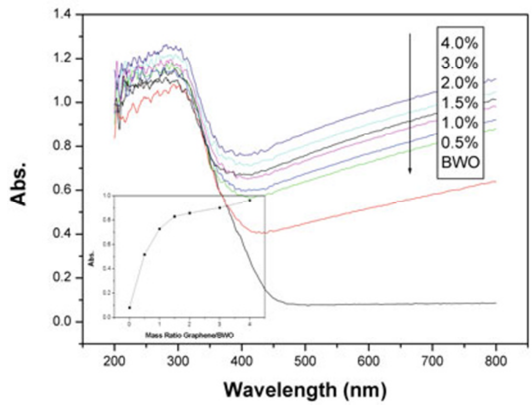

Fig. 4 UV-vis diffuse reflection spectra of BWO and G-BWO samples

The DRS observation and results were consistent to the degradation experiment, and it was speculated that the weight ratio at which nearly compact graphene monolayer coverage was formed on the surface of Bi_2WO_6 was about 1.5 wt%. Graphene may aggregate to form cluster on the surface of Bi_2WO_6 nanoplates when the weight ratio of graphene/Bi_2WO_6 was above 1.5%.

Figure 5 showed the HRTEM structure of Graphene-Bi_2WO_6 photocatalysts. The Bi_2WO_6 nanoplates and 2D graphene nanosheets were clearly observed from Fig. 5a. The image in Fig. 5b showed the intimate contact between graphene and Bi_2WO_6. This intimate contact made the electronic interaction between Bi_2WO_6 and graphene possible, and improved the charge separation efficiency and the photocatalytic activity.

3.3 Mechanism of enhancement of visible photoactivity

It was important to identify the main oxidative species in the photocatalytic degradation process to investigate the photocatalytic mechanism. Detecting the main oxidative species could be carried out through the trapping experiments of radicals and holes [26]. As shown in Fig. 6, the addition of *tert*-butanol as hydroxyl radicals scavenger only caused a minor change in the photocatalytic degradation of MB. On the contrary, the MB could be greatly prevented by the addition of capture for holes (EDTA-Na). It clearly indicated that the free hydroxyl radicals were not the main active oxidative species of the Graphene-Bi_2WO_6 photocatalysts, but the photocatalytic process was mainly governed by direct holes and O_2^- oxidation reaction. It suggested that the oxidative species were not changed after hybridized with graphene.

As discussed above, the electronic interaction between graphene and Bi_2WO_6 was confirmed and the enhanced photocatalytic activity could be explained by the following mechanism: graphene is a good electron acceptor and transporter due to its two-dimensional conjugated π structure, photo-generated electrons can transfer to the graphene. Thus, an effective charge separation is achieved and the possibility of the recombination of electron-hole pairs decreases. Meanwhile, O_2 absorbed on the surface of graphene can accept e^- and form O_2^- which then oxidized MB directly on the surface. As a result, the enhancement of photocatalytic activity can be attributed to a higher separation efficiency for electron-hole pairs, leading to an increase in the number of holes and O_2^- participated in the photooxidation process.

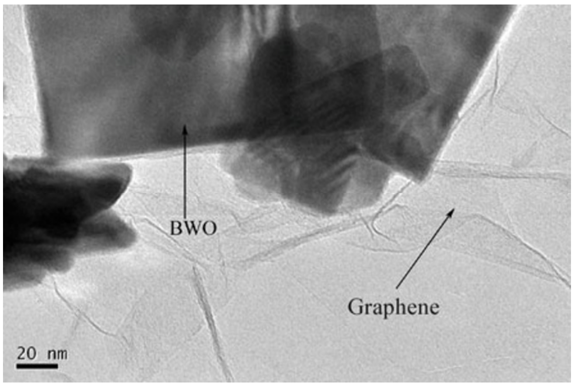

(a)

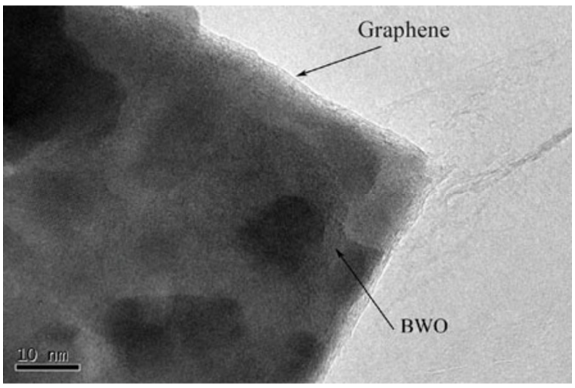

(b)

Fig. 5 HRTEM images of G-BWO composite (1.5 wt%)

4 Conclusions

A graphene-hybridized Bi_2WO_6 photocatalyst (1.5 wt%) showed the highest photocatalytic activity

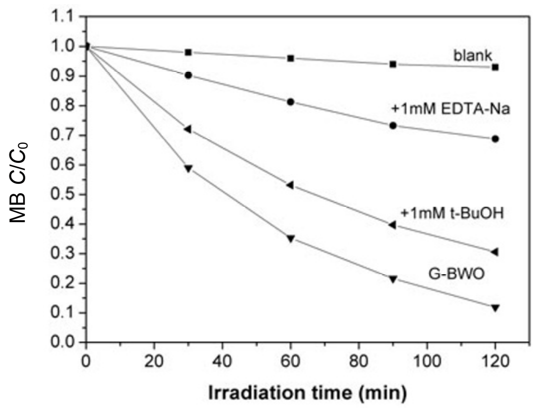

Fig. 6 Photocatalytic degradation of MB with the addition of hole and radical scavenger under visible light irradiation ($\lambda > 420$ nm)

which was about four times of that for pristine Bi_2WO_6 under visible light. A rapid photoinduced charge separation was caused by the hybridization effect between graphene and Bi_2WO_6, which significantly enhanced the activity of the as-prepared Graphene-Bi_2WO_6 photocatalysts. The graphene hybridization was proven to be a promising approach to develop highly efficient and stable photocatalysts under the visible light irradiation.

Acknowledgement

This work was supported by the National Natural Science Foundation of China (20925725), the Fundamental Research Funds for the Central Universities (2011QN138) and State Key Laboratory of New Ceramic and Fine Processing Tsinghua University.

References

[1] Fujishima A, Honda K. Electrochemical photolysis of water at a semiconductor electrode. *Nature* 1972, **238**: 37-38.

[2] Liu GM, Li XZ, Zhao JC. Photooxidation pathway of sulforhodamine-B. dependence on the adsorption mode on TiO_2 exposed to visible light radiation. *Environ Sci Technol* 2000, **34**: 3982-3990.

[3] Asahi R, Morikawa T, Ohwaki T, *et al*. Visible-light photocatalysis in nitrogen-doped titanium oxides. *Science* 2001, **293**: 269-271.

[4] Zhang JY, Zhu HL, Zheng SK, *et al.* TiO_2 Film/Cu_2O microgrid heterojunction with photocatalytic activity under solar light irradiation. *Appl Mater Int* 2009, **1**: 2111-2114.

[5] Tatsuda N, Itahara H, Setoyama N, *et al.* Preparation of titanium dioxide/activated carbon composites using supercritical carbon dioxide. *Carbon* 2005, **43**: 2358-2365.

[6] Zhang XY, Li HP, Cui XL. Preparation and photocatalytic activity for hydrogen evolution of TiO_2/graphene sheets composite. *Chin J Inor Chem* 2009, **25**: 1903-1907.

[7] Chatterjee D, Dasgupta S. Visible light induced photocatalytic degradation of organic pollutants. *J Photochem Photobio C: Photochem Rev* 2005, **6**: 186-192.

[8] Fu HB, Zhang LW, Yao WQ, *et al.* Photocatalytic properties of nanosized Bi_2WO_6 catalysts synthesized via a hydrothermal process. *Appl Catal B: Environ* 2006, **66**: 100-110.

[9] Wu L, Bi JH, Li ZH, *et al.* Rapid preparation of Bi2WO6 photocatalyst with nanosheet morphology via microwave-assisted solvothermal synthesis. *Catal Today* 2008, **131**: 15-20.

[10] Shang M, Wang WZ, Zhang L, *et al.* Bi_2WO_6 with significantly enhanced photocatalytic activities by nitrogen doping. *Mater Chem Phys* 2010, **120**: 155-159.

[11] Woan K, Pyrgiotakis G, Sigmund W. Photocatalytic Carbon-Nanotube-TiO_2 composites. *Adv Mater* 2009, **21**: 2233-2239.

[12] Li YY, Liu JP, Huang XT, *et al.* Carbon-modified Bi_2WO_6 nanostructures with improved photocatalytic activity under visible light. *Dalton Trans* 2010, **39**: 3420-3425.

[13] Zhu SB, Xu TG, Fu HB, *et al.* Synergetic effect of Bi_2WO_6 photocatalyst with C-60 and enhanced photoactivity under visible irradiation. *Environ Sci Technol* 2007, **41**: 6234-6239.

[14] Zhang LW, Fu HB, Zhu YF. Efficient TiO_2 photocatalysts from surface hybridization of TiO_2 particles with graphite-like carbon. *Adv Funct Mater* 2008, **18**: 2180-2189.

[15] Zhang LW, Cheng HY, Zong RL, *et al.* Photocorrosion suppression of ZnO nanoparticles via hybridization with graphite-like carbon and enhanced photocatalytic activity. *J Phys Chem C* 2009, **113**: 2368-2374.

[16] Wang YJ, Shi R, Lin J, *et al.* Significant photocatalytic enhancement in methylene blue degradation of TiO_2 photocatalysts viagraphene-like carbon in situ hybridization. *Appl Catal B: Environ* 2010, **100**: 179-183.

[17] Xu TG, Zhang LW, Cheng HY, *et al.* Significantly enhanced photocatalytic performance of ZnO via graphene hybridization and the mechanism study. *Appl Catal B: Environ* 2011, **101**: 382-387.

[18] Zhou F, Shi R, Zhu YF. Significant enhancement of the visible photocatalytic degradation performances of γ-Bi_2MoO_6 nanoplate by graphene hybridization. *J Mol Catal A: Chem* 2011, **340**: 77-82.

[19] Gao EP, Wang WZ, Shang M, *et al.* Synthesis and enhanced photocatalytic performance of graphene-Bi_2WO_6 composite. *Phys Chem Chem Phys* 2011, **13**: 2887-2893.

[20] Ying H, Wang ZY, Guo ZD, *et al.* Reduced graphene oxide-modified Bi_2WO_6 as an improved photocatalyst under visible light. *Acta Phys Chim Sinica* 2011, **27**: 1482-1486.

[21] Hummers WS, Offeman RE. Preparation of graphitic oxide. *J Am Chem Soc* 1958, **80**: 1339-1339.

[22] Wang D, Choi D, Li J, *et al.* Self-assembled TiO_2-graphene hybrid nanostructures for enhanced Li-Ion insertion. *ACS Nano* 2009, **3**: 907-914.

[23] Li D, Muller MB, Gilje S, *et al.* Processable aqueous dispersions of graphene nanosheets. *Nature Nanotechnology* 2008, **3**: 101-105.

[24] Zhang H, Zong RL, Zhu YF. Photocorrosion inhibition and photoactivity enhancement for Zinc Oxide via hybridization with monolayer polyaniline. *J Phys Chem C* 2009, **113**: 4605-4611.

[25] Cao A, Liu Z, Chu S, *et al.* A facile one-step method to produce Graphene-CdS quantum dot nanocomposites as promising optoelectronic materials. *Adv Mater* 2010, **22**: 103-106.

[26] Xu T, Cai Y, O'Shea KE, *et al.* Adsorption and photocatalyzed oxidation of methylated arsenic species in TiO_2 suspensions. *Environ Sci Technol* 2007, **41**: 5471-5477.